

The Signature of the Stratospheric Brewer-Dobson Circulation in Tropospheric Clouds

Ying Li and David W. J. Thompson

Department of Atmospheric Science, Colorado State University, Fort Collins, CO

1. Introduction

The Brewer-Dobson circulation (BDC) has important implications for global climate. It influences temperatures and concentrations of ozone and water vapor throughout much of the global stratosphere (Brewer 1949; Dobson 1956; Holton *et al.* 1995; Mote *et al.* 1996; Shepherd 2007). The purpose of this study is to demonstrate that variability in the BDC also has a significant influence on clouds at tropospheric levels in two key regions of the atmosphere: the tropical tropopause transition layer (TTL) and the Arctic troposphere.

2. Data and analysis method

The analyses exploit five years (June 2006 through April 2011) of remotely sensed cloud incidence data derived from the merged CALIPSO/CloudSat dataset (Stephens *et al.* 2002). The cloud fraction data are obtained from the Level 2B Geometrical Profiling-LIDAR product (2B-GEOPROF-LIDAR; version P2R04), which combines information from the CloudSat Cloud Profiling Radar (CPR) and CALIPSO lidar.

Instantaneous relationships between cloud incidence and temperature are assessed using the CloudSat European Centre for Medium-Range Weather Forecasts Auxiliary product (ECMWF-AUX). The ECMWF-AUX product is interpolated to the same spatial and temporal resolution sampled by the CloudSat radar. Relationships between cloud incidence and the meteorology on annual and interannual timescales are assessed using the European Centre for Medium Range Weather Forecasts (ECMWF) Interim Reanalysis (ERA-Interim; Simmons *et al.* 2007).

The deep, equator-pole branch of the stratospheric BDC is driven primarily by planetary scale wave breaking in the extratropics (Yulaeva *et al.* 1994; Holton *et al.* 1995; Ueyama and Wallace 2010; Zhou *et al.* 2012; Grise and Thompson 2012). The planetary wave entering in the extratropical stratosphere can be measured by the vertical flux of wave activity in the lowermost stratosphere (*e.g.*, Waugh *et al.* 1999; Newman *et al.* 2001; Randel *et al.* 2002a; Polvani and Waugh 2004), which is proportional to the zonal-mean meridional eddy flux of heat at 100 hPa: $[\overline{v^*T^*}]_{100\text{hPa}}$, where the brackets denote the zonal mean and asterisks denote the deviation from zonal mean. As the planetary-scale wave-driven BDC has largest amplitude in the Northern Hemisphere (NH) and during boreal winter (*e.g.*, Yulaeva *et al.* 1994; Rosenlof 1995), we focus on the wave fluxes averaged poleward of 30°N ($[\overline{v^*T^*}]_{100\text{hPa}, 30-90^\circ\text{N}}$), and regressions on the wave fluxes are centered on the months October–March. The fluxes are calculated from six hourly v and T and then averaged to form monthly means.

As on month-to-month timescales, stratospheric wave driving is correlated with temperatures during both the current and subsequent month, we define our index of the BDC as weighted average of $([\overline{v^*T^*}]_{100\text{hPa}, 30-90^\circ\text{N}})$ formed from the previous and current months values. The corresponding weights are determined via an empirical fit of the $([\overline{v^*T^*}]_{100\text{hPa}, 30-90^\circ\text{N}})$ time series to lowermost stratospheric temperatures. As noted in Ueyama and Wallace (2010), the weights applied to the previous and current months values of $[\overline{v^*T^*}]_{100\text{hPa}, 30-90^\circ\text{N}}$ are roughly 2 and 1, respectively. That is, the BDC index value for month i is defined as:

$$\text{BDC}(i) = 2 \times [\overline{v^*T^*}]_{100\text{hPa}, 30-90^\circ\text{N}}(i-1) + 1 \times [\overline{v^*T^*}]_{100\text{hPa}, 30-90^\circ\text{N}}(i),$$

where (i) is the current month, and ($i - 1$) is the previous month. The resulting BDC index time series is then standardized so that it is dimensionless. The standardized BDC index is hereafter referred to as BDC_{NH} .

3. Results

We will first establish the robustness of the linkages between cloud incidence and tropopause temperatures in both these regions. We will then draw on the inferred linkages to motivate and support the analyses between cloud incidence and stratospheric wave driving.

3.1. Cloud incidence as a function of SST and tropopause temperature

The left and middle panels in Figure 1 examine the vertical distribution of cloud incidence over the tropical ocean as a function of sea-surface temperature (SST; Fig. 1a) and over the tropical ocean and land as a function of tropopause temperature (Fig. 1b). The right panel examines the vertical distribution of cloud incidence as a function of tropopause temperatures over the Arctic poleward of 60°N (Fig. 1c). The key results in Figure 1 are strong linkages between tropopause temperatures and upper tropospheric clouds at both tropical and NH polar latitudes.

The linkages between tropopause temperatures and upper tropical tropospheric clouds (Fig. 1b) are in part due to the coherence between tropopause temperatures and SSTs: regions of anomalous SSTs force large-scale equatorial waves, and such waves influence TTL temperatures and cirrus through adiabatic motions (*e.g.*, Boehm and Lee 2003; Norton 2006; Virts *et al.* 2010). To test the independent relationship between tropical tropopause temperatures and cloud

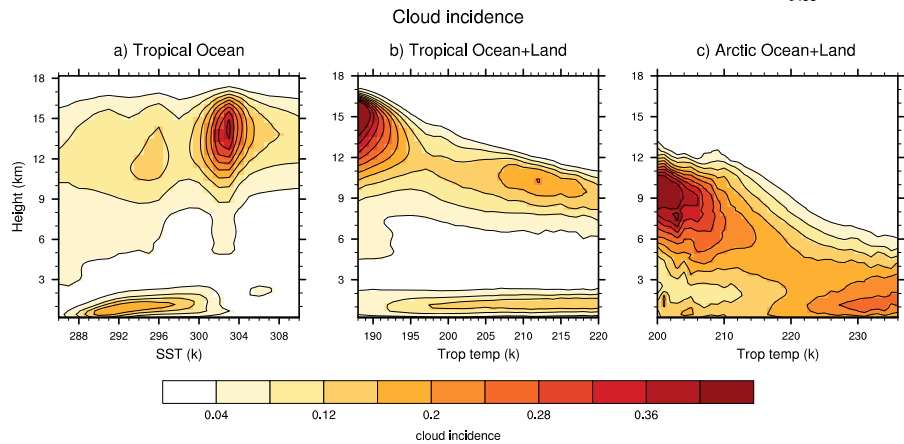


Fig. 1 Cloud incidence (shading) as a function of height and (a) sea-surface temperature (SST) over the tropical ocean, (b) tropopause temperature over the tropical ocean and land, and (c) tropopause temperature over the Arctic poleward of 60°N . Results are based on contemporaneous relationships between cloud incidence from CloudSat/CALIPSO product sea-surface and tropopause temperatures from the ECMWF-AUX product. The seasonal cycle is not removed from the data. All satellite swaths from June 2006 through April 2011 are used. There are a total of more than 2×10^8 individual profile measurements over the tropics, and more than 9×10^7 individual profile measurements over the Arctic. The bin size in all plots is 1 K.

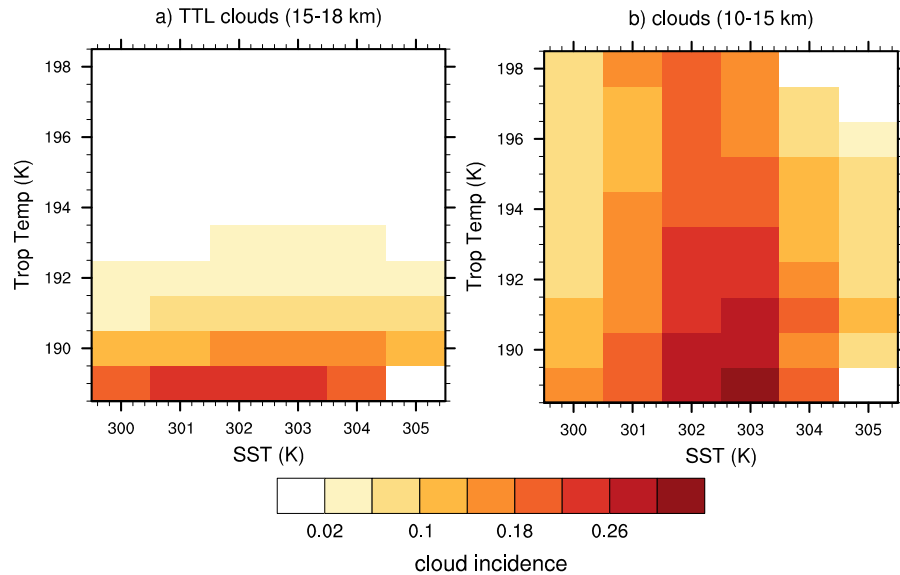


Fig. 2 Cloud incidence (shading) over the tropical ocean shown as a function of SST and tropopause temperature. Results are shown for cloud incidence averaged between (a) 15–18 km and (b) 10–15 km. Results are based on data for all months of the year, and are focused on regions where SSTs are higher than 300 K and tropopause temperatures are lower than 198 K. The seasonal cycle is not removed from the data. The bin size in all plots is 1 K.

incidence, we show in Figure 2 the incidences of clouds between 15–18 km (top) and 10–15 km (bottom) as a function of sea-surface (abscissa) and tropopause temperature (ordinate). The 15 km level corresponds roughly to the base of TTL (*e.g.*, Shepherd 2007; Fueglistaler *et al.* 2009). Cloud incidence between 15–18 km (Fig. 2 top) is clearly a much stronger function of tropopause temperature than of SST, whereas tropical cloud incidence between 10–15 km (Fig. 2 bottom) is a function of both tropopause and sea-surface temperature.

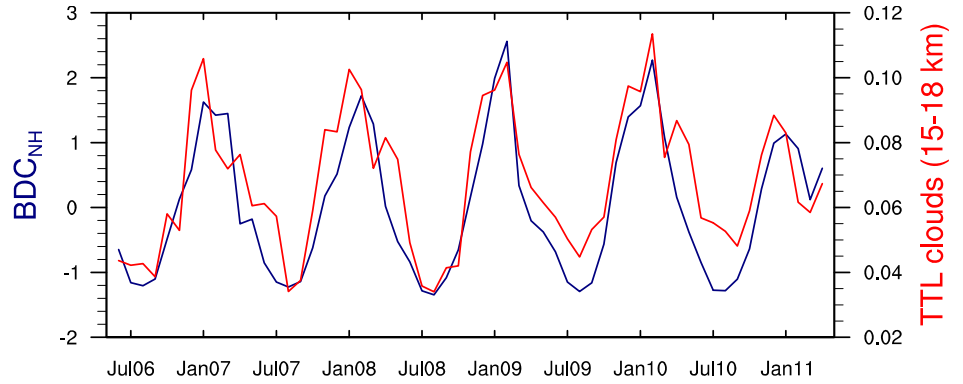


Fig. 3 Monthly-mean cloud incidence averaged 30°S–30°N and between 15–18 km (red; scale at right) and the standardized BDC_{NH} index (blue; scale at left). The BDC_{NH} index is based on the meridional eddy flux of heat and is defined in Section 2.2.

3.2 The signature of Brewer-Dobson circulation in TTL cirrus and Arctic tropospheric clouds

In this section we will build on the relationships between tropopause temperature and cloud incidence established in Figures 1–2 to demonstrate a robust link between the stratospheric Brewer-Dobson circulation and clouds in both the TTL and Arctic troposphere. The BDC index (BDC_{NH}) is based on the vertical flux of wave activity into the NH extratropical stratosphere during winter and is described in Section 2. Figure 3 confirms the coherence between the annual cycles of NH stratospheric wave driving and cloud incidence in the TTL, and support Virts and Wallace (2010)’s conclusion that the large-scale BDC plays a central role in the seasonal cycle of TTL cirrus.

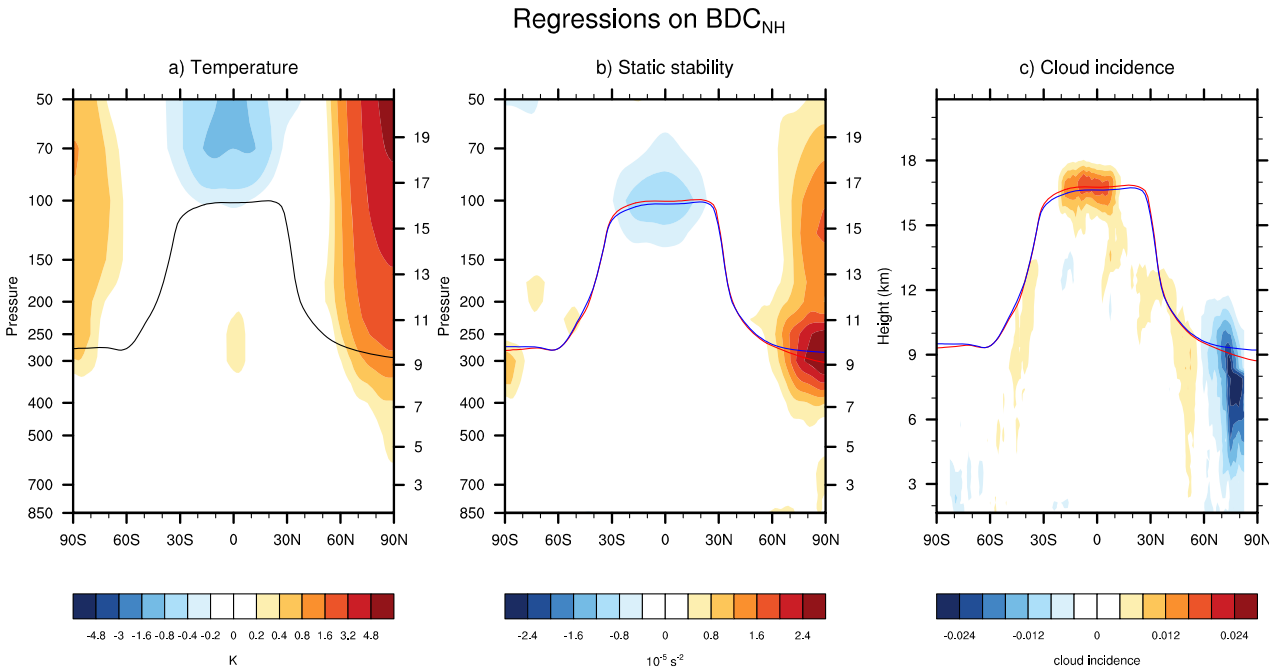


Fig. 4 Regressions of zonal-mean (a) temperature, (b) static stability and (c) cloud incidence onto standardized monthly-mean values of the anomalous BDC_{NH} index. Results are shown as a function of latitude and height and are based on October–March data from June 2006–April 2011. The seasonal cycle has been removed from the data. Units are K (temperature) and $10^{-4} s^{-2}$ (static stability). The solid black line in (a) corresponds to the climatological-mean (October–March) tropopause height. The red and blue lines in (b) and (c) indicate the climatological-mean tropopause height plus and minus the regression of tropopause height onto the standardized BDC_{NH} index, respectively.

Figures 4–5 examine the linkages between the BDC, atmospheric temperatures and tropospheric clouds on month-to-month timescales during the NH winter months October–March. Figure 4a shows monthly-mean, zonal-mean temperature anomalies regressed on standardized wintertime values of the anomalous BDC_{NH} index. The solid black line indicates the climatological-mean (October–March) tropopause height. Periods of enhanced wave driving in the extratropical stratosphere are associated with anomalously low temperatures in the tropical lower stratosphere and anomalously high temperatures in the polar stratosphere.

Figure 4b shows the corresponding changes in atmospheric static stability. Here the red and blue lines indicate the climatological-mean tropopause height plus (red) and minus (blue) the regression of tropopause height onto the wintertime values of the BDC_{NH} index. Periods of enhanced stratospheric wave driving lead to 1) anomalously high tropopause heights and anomalously low static stability at ~ 100 hPa in the tropics juxtaposed against 2) anomalously low tropopause heights and anomalously high static stability in the upper troposphere/lower stratosphere in the Arctic.

Figure 4c shows the corresponding changes in cloud incidence. Month-to-month variability in stratospheric wave driving is associated with a distinct pattern of near-tropopause cloudiness. Periods of enhanced stratospheric wave driving are marked by anomalously high cloud incidence near the tropical tropopause and anomalously low cloud incidence near the Arctic tropopause. The anomalies in tropical cloud incidence are limited to the tropopause region, whereas the anomalies in Arctic cloud incidence extend to the middle-upper troposphere.

The linkages between the BDC and cloud incidence revealed in Fig. 4c also highly significant. As shown in Figure 5, variability in the BDC accounts for more than 25% of the month-to-month variability in cloudiness in both the TTL and Arctic troposphere. The associated correlation coefficients are significant at the 99% confidence level based on a one-tailed test of the t -statistics with an effective sampling size of 24 (using the criterion given in Bretherton *et al.* 1999).

4. Concluding remarks

The planetary-scale stratospheric Brewer-Dobson circulation influences temperatures and static stability in the vicinity of the tropopause in both the tropics and Arctic. Periods of enhanced wave driving in the NH extratropical stratosphere are marked by lifting and cooling of the tropical tropopause juxtaposed against sinking and warming of the Arctic tropopause, and vice versa. Here we exploited ~ 5 years of data from the CloudSat and CALIPSO instruments to reveal that the influence of the BDC during NH winter extends to clouds in both the TTL and Arctic troposphere. The BDC accounts not only for the seasonal cycle in TTL cirrus [Fig. 3; Virts and Wallace 2010], but also for $\sim 25\%$ of the month-to-month variability in cloud incidence in both the TTL and Arctic troposphere during NH winter (Figs. 4c, 5). The results reveal a novel pathway through which stratospheric processes can influence tropospheric climate.

The linkages between the BDC and clouds in the TTL and Arctic troposphere are physically plausible and statistically robust. Upper tropospheric cloud incidence is linked to variability in tropopause temperatures in both the tropics and over the Arctic (Figs. 1, 2). Tropopause temperatures and static stability in both regions

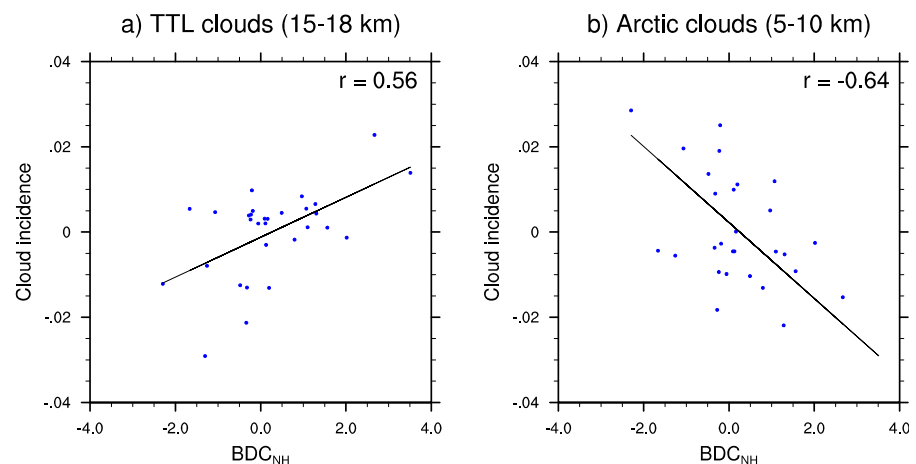


Fig. 5 Scatterplots of monthly mean values of the anomalous BDC_{NH} index (abscissa) and cloud incidence (ordinate). Cloud incidence is averaged (a) equatorward of 30° and between 15–18 km and (b) poleward of $60^\circ N$ and between 5–10 km. Results are based on October–March data from June 2006–April 2011.

are, in turn, linked to variability in the BDC (Figs. 4a, 4b). The subsequent linkages between variability in the BDC and clouds in the TTL and Arctic troposphere are significant at the 99% level (Fig. 5).

The linkages between the BDC and clouds in the TTL and Arctic troposphere have potential implications for both climate change and the ability of models to simulate such change. Climate change simulations reveal robust increases in the strength of the BDC in response to future increases in greenhouse gases (*e.g.*, Butchart and Scaife 2001; Butchart *et al.* 2006; Li *et al.* 2008; Garcia and Randel 2008; McLandress and Shepherd 2009; Butchart *et al.* 2010), and at least some observations suggest that such changes have already occurred (Thompson and Solomon 2009; Hu and Fu 2009; Young *et al.* 2012). The changes in cloudiness associated with a strengthening of the BDC may have notable radiative effects on both the TTL and Arctic troposphere. The radiative effects of the linkages documented here and the ability of climate models to simulate such linkages remain to be determined.

References

- Boehm, M. T. and S. Lee, 2003: The implications of tropical Rossby waves for tropical tropopause cirrus formation and for the equatorial upwelling of the Brewer-Dobson circulation. *J. Atmos. Sci.*, **60**, 247–261.
- Bretherton, C. S., M. Widmann, V. P. Dymnikov, J. M. Wallace, and I. Bladé, 1999: The effective number of spatial degrees of freedom of a time-varying field. *J. Climate*, **12**, 1990–2009.
- Brewer, A. W., 1949: Evidence for a world circulation provided by the measurements of helium and water vapor distribution in the stratosphere. *Quart. J. Roy. Meteor. Soc.*, **75**, 351–363.
- Butchart, N. and A. A. Scaife, 2001: Removal of chlorofluorocarbons by increased mass exchange between the stratosphere and troposphere in a changing climate. *Nature*, **410**, 799–802.
- Butchart, N., and Co-authors, 2006: Simulations of anthropogenic change in the strength of the Brewer-Dobson circulation. *Climate Dyn.*, **27**, 727–741.
- Butchart, N., and Co-authors, 2010: Chemistry-climate model simulations of 21st century stratospheric climate and circulation changes. *J. Climate*, **23**, 5349–5374, doi:10.1175/2010JCLI3404.1.
- Dobson, G. M. B., 1956: Origin and distribution of polyatomic molecules in the atmosphere. *Proc. Roy. Soc. London.*, **A236**, 187–193.
- Fueglistaler, S., A. E. Dessler, T. J. Dunkerton, I. Folkins, Q. Fu, and P. W. Mote, 2009: Tropical tropopause layer. *Rev. Geophys.*, **47**, RG1004, doi:10.1029/2008RG000267.
- Garcia, R. R. and W. J. Randel, 2008: Acceleration of the Brewer-Dobson circulation due to increases in greenhouse gases. *J. Atmos. Sci.*, **65**, 2731–2739.
- Grise, K.M. and D.W. J. Thompson, 2012: On the signatures of equatorial and extratropical wave forcing in tropical tropopause layer temperatures. *J. Atmos. Sci.*, in press.
- Holton, J. R., P. H. Haynes, M. E. McIntyre, A. R. Douglass, R. B. Rood, and L. Pfister, 1995: Stratosphere-troposphere exchange. *Rev. Geophys.*, **33**, 403–439.
- Hu, Y. and Q. Fu, 2009: Stratospheric warming in Southern Hemisphere high latitudes since 1979. *Atmos. Chem. Phys.*, **9**, 4329–4340, doi:10.5194/acp-9-4329-2009.
- Li, F., J. Austin, and R. J. Wilson, 2008: The strength of the Brewer-Dobson circulation in a changing climate: Coupled chemistry-climate model simulations. *J. Climate*, **21**, 40–57.
- Lin, P., Q. Fu, S. Solomon, and J. M. Wallace, 2009: Temperature trend patterns in Southern Hemisphere high latitudes: Novel indicators of stratospheric change. *J. Climate*, **22**, 6325–6341.
- McLandress, C. and T. G. Shepherd, 2009: Simulated anthropogenic changes in the Brewer-Dobson circulation, including its extension to high latitudes. *J. Climate*, **22**, 1516–1540.
- Mote, P. W., et al., 1996: An atmospheric tape recorder: The imprint of tropical tropopause temperatures on stratospheric water vapor. *J. Geophys. Res.*, **101**, 3989–4006, doi:10.1029/95JD03422.
- Newman, P. A., E. R. Nash, and J. E. Rosenfield, 2001: What controls the temperature of the Arctic stratosphere during the spring? *J. Geophys. Res.*, **106**, 19 999–20 010.

- Norton, W. A., 2006: Tropical wave driving of the annual cycle in tropical tropopause temperatures. Part II: Model results. *J. Atmos. Sci.*, **63**, 1420–14 331.
- Polvani, L. M. and D. W. Waugh, 2004: Upward wave activity flux as precursor to extreme stratospheric events and subsequent anomalous weather regimes. *J. Climate*, **17**, 3548–3554.
- Randel, W. J., F. Wu, and R. Stolarski, 2002: Changes in column ozone correlated with the stratosphere EP flux. *J. Meteor. Soc. Japan*, **80**, 849–862.
- Rosenlof, K. H., 1995: Seasonal cycle of the residual mean meridional circulation in the stratosphere. *J. Geophys. Res.*, **100**, 5173–5191.
- Shepherd, T. G., 2007: Transport in the middle atmosphere. *J. Meteor. Soc. Japan*, **85B**, 165–191.
- Simmons, A., S. Uppala, D. Dee, and S. Kobayashi, 2007: ERA-Interim: New ECMWF re-analysis products from 1989 onwards. *ECMWF Newsletter*, **110**, 25–35, ECMWF, Reading, United Kingdom.
- Stephens, G. L. and Coauthors, 2002: The CloudSat mission and the A-train: A new dimension of space-based observations of clouds and precipitation. *Bull. Amer. Meteor. Soc.*, **83**, 1771–1790, doi:10.1175/BAMS-83-12-1771.
- Thompson, D. W. J. and S. Solomon, 2009: Understanding recent stratospheric climate change. *J. Climate*, **22**, 1934–1943.
- Ueyama, R., and J. M. Wallace, 2010: To what extent does 485 high latitude wave forcing drive tropical upwelling in the Brewer-Dobson circulation? *J. Atmos. Sci.*, **67**, 1232–1246.
- Virts, K. S., J. M. Wallace, Q. Fu, and T. P. Ackerman, 2010: Tropical tropopause transition layer cirrus as represented by CALIPSO lidar observation. *J. Atmos. Sci.*, **67**, 3113–3129.
- Waugh, D., W. Randel, S. Pawson, P. Newman, and E. Nas, 1999: Persistence of the lower stratospheric polar vortices. *J. Geophys. Res.*, **104**, 27191–27201.
- Young, P. J., K. H. Rosenlof, S. Solomon, S. C. Sherwood, Q. Fu, and J.-F. Lamarque, 2012: Changes in stratospheric temperatures and their implications for changes in the BrewerDobson circulation. *J. Climate*, **25**, 1759–1772, doi:10.1175/2011JCLI4048.1.
- Yulaeva, E., J. Holton, and J. M. Wallace, 1994: On the cause of the annual cycle in tropical lower-stratospheric temperatures. *J. Atmos. Sci.*, **51**, 169–174.
- Zhou, T., M. A. Geller, and W. Lin, 2012: An observational study on the latitudes where wave forcing drives Brewer-Dobson upwelling. *J. Atmos. Sci.*, **69**, 1916–1935.